International Journal of Nanomedicine

Dovepress
open access to scientific and medical research

Open Access Full Text Article

ORIGINAL RESEARCH

Antiviral Activity of Zinc Oxide Nanoparticles Mediated by *Plumbago indica* L. Extract Against Herpes Simplex Virus Type 1 (HSV-1)

Mina Michael Melk[1]
Seham S El-Hawary[1]
Farouk Rasmy Melek[2]
Dalia Osama Saleh[3]
Omar M Ali[4]
Mohamed A El Raey[5]
Nabil Mohamed Selim[1]

[1]Pharmacognosy Department, Faculty of Pharmacy, Cairo University, Giza, Egypt; [2]Chemistry of Natural Compounds Department, National Research Centre, Giza, Egypt; [3]Pharmacology Department, National Research Centre, Giza, Egypt; [4]Department of Chemistry, Turabah University College, Turabah Branch, Taif University, Taif, 21944, Saudi Arabia; [5]Department of Phytochemistry and Plant Systematics, Pharmaceutical Division, National Research Centre, Dokki, Cairo, Egypt

Introduction: *Plumbago indica* L. is considered a valuable source in the Plumbaginaceae family for various types of active compound such as alkaloids, phenolics and saponins. To promote the usage of *P. indica* in the bionanotechnology field, zinc oxide nanoparticles (ZnONPs) were biosynthesized by using its alcoholic extract. The inhibitory effects of ZnONPs and the plant extract were also evaluated against HSV-1.

Methods: ZnONPs were described by the following techniques, UV–visible spectroscopy, Fourier transform infrared spectroscopy (FTIR), dynamic light scattering (DLS), zeta potential, scanning electron microscopy (SEM), transmission electron microscopy (TEM) and x-ray diffraction (XRD). The phenolic and flavonoid contents of *P. indica* extract, which are accountable for bioreduction, formation and stabilization of the nanoparticles, were analyzed by HPLC technique. The antiviral assessment was implemented on both agents by using Vero cell lines.

Results: DLS revealed that the average size of ZnONPs was 32.58 ± 7.98 nm and the zeta potential was –20.8 mV. The observation of TEM analysis revealed that the particle size of ZnONPs varied from 2.56 to 8.83 nm. The XRD analysis verified the existence of pure crystals of hexagonal shapes of nanoparticles of ZnO with a main average size of 35.28 nm that is approximating to the values of particle size acquired by SEM analysis (19.64 and 23.21 nm). The HPLC analysis of *P. indica* ethanolic extract showed that gallic acid, chlorogenic acid and rutin were the major compounds, with concentrations equal to 8203.99, 2965.95 and 1144.99 µg/g, respectively. Regarding the antiviral assessment, the synthesized uncalcinated ZnONPs were found to exhibit a promising activity against HSV-1, with CC_{50} and IC_{50} values equal to 43.96 ± 1.39 and 23.17 ± 2.29 µg/mL, respectively.

Conclusion: The green synthesized ZnONPs are considered promising adjuvants to enhance the efficacy of HSV-1 drugs.

Keywords: ZnO nanoparticles, *Plumbago indica* L., HPLC analysis, antiviral activity and green synthesis

Introduction

The nanoparticles of metal oxide possess valuable physical, chemical, and biological properties and are considered a promising tool used in various applications.[1] In the process of nanoparticle synthetization, numerous side effects are arising due to the usage of toxic chemicals acting as reductive and capping agents. However, the utilization of numerous natural extracts, particularly plant extracts, in the metal oxide nanoparticles synthesis has received attention. This is because the natural approach is time saving and ecofriendly compared to the other conventional methods; also, the occurrence of several bioactive phytochemicals assists in the

Correspondence: Nabil Mohamed Selim; Omar M Ali
Email nabil.selim@pharma.cu.edu.eg; om.ali@tu.edu.sa

Received: 6 October 2021
Accepted: 5 December 2021
Published: 18 December 2021

reduction and stabilization of nanomaterials.[2] Recently, scientists have recognized the importance of zinc oxide (ZnO) due to its plentiful applications and unique properties.[3–6] The nanoparticles containing ZnO have an important role in avoidance of the aquatic and dependent ecosystem imbalances arising from organic contaminants such as dye fragments. ZnONPs synthesized by *Artocarpus heterophyllus* leaves were effective in degradation of Congored dye.[7] ZnO nanorods produced by *Calotropis gigantea* were proved to act as a photo catalyst in the degradation process of titan yellow dye.[8] Also, the ZnONPs application at concentration of 100 μg mL^{-1} protects plants from tobacco mosaic virus infection.[9]

Reviewing previous reports, ZnONPs were successfully synthesized from numerous natural extracts as *Aloe vera*,[10] *Passiflora caerulea*[11] and *Azadirachta indica*.[12,13] Furthermore, ZnONPs have received much attention and are presently applied in numerous fields such as packaging and food additives. Among other types of nanoparticle, ZnONPs become absorbed easily by the biological tissues and have a good biocompatibility with human cells more than zinc metal. Additionally, ZnONPs demonstrate an antiviral activity against many viruses such as various types of respiratory viruses and herpes viruses, including SARS-CoV-2.[14] There are several mechanisms for the antiviral activity of ZnONPs, such as prevention of viral entry, viral replication and spreading to organs, which can eventually trigger reactive oxygen species leading to oxidative injury and viral death.[14] Zinc containing compounds revealed antiviral activity against numerous viruses by different mechanisms such as physical processes including attachment to virus, inhibition of virus infection, and uncoating. Also, these compounds showed activity by biological mechanisms such as inhibition of viral polymerases and protease enzymes.[9]

Generally, Zn is an important component that occurs in human tissue such as the bone, brain, muscle and skin. This vital element is also involved in various enzyme processes such as metabolism and protein and nucleic acid biosynthesis.[15]

It is worth noting that the US Food and Drug Administration (FDA) categorized ZnO as a nontoxic substance. Therefore, ZnONPs are allowed to be applied in numerous biomedical activities. ZnONPs are characterized by their low toxicity and cost effectiveness and therefore can be applied in numerous therapeutic fields, such as wound healing and drug delivery, and for anticancer, antidiabetic, antibacterial and anti-inflammatory purposes.[15]

Plumbago indica L. belongs to the largest genus of flowering plant in the family Plumbaginaceae. This plant, previously known as *P. rosea*, can grow in diverse regions of Southeast Asia, Europe, Malaysia, Indonesia, Africa, China and India.[16] *P. indica* contains various types of constituent, such as apigenin, kaempferol, luteolin, plumbaginol, myricetin tetra methyl ether, ampelopsin tetramethylether, Plumbagin-5-*O*-α-L-Rhamnopyranoside, campesterol, β-sitosterol and stigmasterol.[17,18] Among numerous *Plumbago* species, *P. indica* contains a high amount of plumbagin.[19] Numerous pharmacological activities for plumbagin were reported, such as antioxidant,[20] antimicrobial,[21] and anticancer[22] activities.

The interactions between nanoparticles and biological targets have revolutionized the field of drug development.[23] Selenium NPs play important roles in various medical applications such as anticancer, antitumor, antibacterial and antiviral agents. They boost drug and gene delivery and show synergistic properties.[24] The micro and nano ZnO particles exhibit highly promising prophylactic agents against HSV-1[25] and PEGylation of these nanoparticles causes reduction of the cytotoxic effect and enhances their antiviral efficacy.[26] Numerous metal NPs were successfully ecofriendly synthesized by different *Plumbago* species and found to have various biological activities. Sliver NPs were previously green-synthesized using various *Plumbago* species such as *P. indica, P. auriculata*, and *P. zeylanica* and proved to possess antioxidant, antitumor, antibacterial, larvicidal and antitubercular properties.[27–30] *P. zeylanica* was used to synthesize selenium, copper, silver, gold, and bimetallic (silver and gold) NPs. These nanoparticles were found to exhibit antioxidant, antibacterial,[31] antidiabetic,[32] antimicrobial and antibiofilm effects.[33] Highly stable ZnONPs were also obtained from *P. zeylanica* extract and were found to have antibacterial activity against *Staphylococcus aureus and Salmonella typhimurium*.[34] ZnONPs synthesized from *P. auriculata* alcoholic extract demonstrated an antiviral effect against avian metapneumovirus subtype B.[35]

Most of the investigations done on the antimicrobial activity of ZnONPs focused on the antibacterial effects and there are limited studies dealing with interaction between ZnONPs or *P. indica* extract and viruses.

The current study aimed to inspect the effect of ZnONPs produced by alcoholic extract of *P. indica* against HSV-1. Furthermore, the phytochemical constituents present in this extract are characterized by HPLC technique.

Materials and Methods

Plant Material

Flowering aerial parts of *P. indica* were procured from EL -MAZHAR botanical garden, Giza, Egypt. The plant was kindly authenticated by Engineering Therease Labib Consultant for plant identification at El-Orman botanical garden, Giza and Dr. Mohamed El Gebaly, Botany Taxonomist at National Research Centre Herbarium, Dokki, Giza. Voucher specimen (numbered 19062020) was reserved at the herbarium of the Department of Pharmacognosy, Faculty of Pharmacy, Cairo University. *P. indica* flowering aerial parts were air-dried, coarsely powdered and preserved in tightly closed amber-colored glass containers at room temperature. This research was performed in accordance with the guidelines of occupational health and safety committee at National Research Centre, Giza, Egypt and accepted by scientific research ethics committee of Faculty of Pharmacy, Cairo University, Giza, Egypt.

Extraction of Plant Active Ingredients

The air-dried powder of the flowering aerial parts of *P. indica* (100 g) were successfully extracted by maceration technique with 90% ethanol (250 mL. × 3). The obtained extract was evaporated using Buchi Rotary Evaporators under reduced pressure till dryness (2.5 g.).

HPLC Analysis

HPLC analysis was performed by means of an Agilent 1260 series. The separation column was Eclipse C18 column (4.6 mm x 250 mm i.d., 5 µm). The mobile phase was comprised of (A) water and (B) 0.05% trifluoroacetic acid in acetonitrile using a flow rate of 1 mL/min. The mobile phase was automatic flow in a linear gradient as follows: 0 min (82% A and 18% B); 0–5 min (80% A and 20% B); 5–12 min (60% A and 40% B) and 12–16 min (82% A and 18% B). The detector used was multi-wavelength and adjusted at 280 nm. The injection volume was 10 µL for the standard and extract solutions. The column temperature was set at 35 °C.

Green Synthesis of Zinc Oxide Nanoparticles

ZnONPs were synthesized from the alcoholic extract of the flowering aerial parts of *P. indica* by a method illustrated previously by Attia et al,[36] with slight modification in which *P. indica*. dried extract (1 g) was dissolved in ethanol (100 mL) reacted with zinc acetate (10 g) dissolved in doubly distilled water (1000 mL) and heated in water bath for 20 min at 100 °C. Ammonium hydroxide (a few drops) was added to the reactant media to maintain pH at 12, in which ZnONPs precipitate is created. The mixture was set for 60 minutes for complete reduction of zinc acetate to ZnONPs. The obtained ZnONPs was centrifuged at 4000 rpm, followed by washing in bi-distilled water (twice) and ethanol (twice) to yield white pellets of nanoparticles upon freeze drying.

Characterization of Metal Nanoparticles

The ZnONPs were initially analyzed by means of UV-1601 (Shimadzu Corporation, Japan) UV–visible spectroscopy ranging between 200 and 600 nm. Then, FTIR analysis using attenuated total reflectance mode by a Jasco FTIR 4100 spectrophotometer (Japan) was applied to categorize the functional groups and various phytochemical compounds responsible for formation and stabilization of the nanoparticles. Dynamic light scattering (DLS) analysis obtained by a Zetasizer (HT Laser, ZEN3600, Malvern Instruments, Malvern, UK) was applied to investigate particle size and zeta potential of the nanoparticles. Morphology and particle size of ZnONPs mediated by *P. indica* extract was determined by TEM (JEOL-JEM-1011, Japan) and FE-SEM (Mira3 Tescan). A few drops from the suspension of ZnO nanoparticles were applied to a carbon-coated copper grid and the solvent was evaporated at room temperature prior to recording the images. The powdered sample was also subjected to CuKα1-X Ray diffractometer radiation (λ = 1.5406 A°) operating at 40 kV and 30 mA with 2θ ranging from 20–90° to verify the occurrence of ZnO crystals and define their structure and size.

Evaluation of the Antiviral Activity of ZnONPs and *P. indica*

The antiviral assessment of ZnONPs and *P. indica* extract was performed by plaque inhibition assay using Vero cells (ATCC, Manassas, VA, USA) acquired from the kidneys of African green monkey, Herpes Simplex Virus type 1 (EA2387, Hopital PitiéSalpétrière, France) and acyclovir as standard reference drug. The proliferation of the Vero cells line and the preparation of the virus stock were performed according to El-Toumy et al[37] and stored at −70°C until used. Virus titrations were calculated from cytopathogenicity and directly related to the 50% of

infectious doses per milliliter ($2 \times 10^{7.4}$ ID_{50}/mL) according to the Reed and Muench dilution method.[38]

Cytotoxicity Assay

The cytotoxicity of the investigated agents was assessed by neutral red dye-uptake technique as previously reported.[39] Briefly, the test compounds and acyclovir were diluted in 0.1% dimethyl sulfoxide (DMSO). Stock solutions at a concentration of 200 µg/mL were prepared by 0.1% DMSO. Vero cell monolayers cultivated with investigated agents or the positive control (two-fold serial dilutions each) were incubated for 72 h at 37◦C in 5% CO_2 using Eagle's MEM containing 8% FCS. After incubation, the alterations in cellular morphology were visualized by means of an inverted optical microscope for determination of MNTC (maximum non-toxic concentrations). The CC50 values (concentrations of each agent essential for reduction of cell viability by 50%) were computed by comparing with the untreated cells. The cytotoxicity of compounds active against HSV-1 was also assessed in triplicate to obtain statistically relevant data for final calculations.

Anti-herpes Simplex Virus Type 1 (HSV-1) Assay

Each well in a 96-well plate containing Vero cellular suspension (100 µL, 3.5×10^5 cells/mL) and investigated agents (50 µL) was infected with viral suspension (50 µL) at MOI (multiplicity of infection) of 0.001 ID_{50}/cells. The plate was then incubated for 3 days at 37°C in 5% CO_2 without changing the media. Blanks for virus and cell were run simultaneously. After the viral growth, the cultures were stained with neutral red dye (50 µL, 0.15% in saline, pH 5.5) and incubated for 45 min at 37°C.[40] Phosphate buffered saline (pH 7.2) was used for removing excess dye while the elution of the dye attached in the viable cells was performed using citrate ethanol buffer (100 µL/well). The anti-herpetic compound acyclovir was used with concentrations ranging from 0.5 to 5 µg/mL. The cell culture monolayer was completely destroyed after shaking the plate for 20 min. The absorbance (OD) of each well was recorded using a multichannel spectrophotometer at 540 nm. The OD was directly proportional to the percentages of viable cells that were inversely related to the cytopathic effect (CPE) ratio. The values of CC_{50} and IC_{50} of all the investigated agents were computed from the regression straight line of each assay that was obtained on the basis of virus controls (100% CPE) and cell controls (0% CPE).[41] The percentage of protection (%P) was calculated by the following formula: (no%P = [(A1) − (A2)]/[(A3) − (A2)] × 100) where (A1) is the absorbance of the test sample, (A2) is the absorbance of the virus-infected control and (A3) is the absorbance of the mock-infected control. The ratio of (A2) to (A3) is expressed as "% of control".

Statistical Analysis

GraphPad PRISM software V.5 was used for calculations and statistical analysis. The values of mean and standard deviations (SDs) for each experiment were calculated. ANOVA followed by Tukey's multiple comparison test was used to obtained the significance between the tested agents and the positive control.

Results and Discussion

HPLC Analysis of Phenolic Compounds

HPLC analysis (Figure 1) revealed the occurrence of 15 compounds in the alcoholic extract of the aerial parts of *P. indica*. The HPLC analysis of this extract showed that gallic acid, chlorogenic acid and rutin were the major compounds, with concentrations equal to 8203.99, 2965.95 and 1144.99 µg/g, respectively (Table 1). The rest of the compounds were characterized as catechin, methyl gallate, caffeic acid, syringic acid, rutin, ellagic acid, coumaric acid, vanillin, ferulic acid, naringenin, taxifolin and cinnamic acid and are reported here for the first time. Kaempferol was previously reported as kaempferol–3–*O*–rhamnoside from *P. indica* L. flowers.[42] To the best of our knowledge, this is the first approach for identification of phenolic compounds using the HPLC technique.

ZnO Nanoparticle Formation

P. indica L. alcoholic extract reacted with zinc acetate solution in hot water bath at 80°C. Addition of ammonium hydroxide to the reaction mixture precipitated ZnONPs (Figure 2).[36]

ZnONPs Characterizations

UV Analysis

A maximum absorption peak of ZnONPs synthesized from *P. indica* extract was found at 368 nm (Figure 3), indicating the ZnONPs formation.[43] The broadness of absorption could be attributed to the transition of the electronic cloud on the overall skeleton of the ZnONPs.[44] At a nano scale, ZnO has

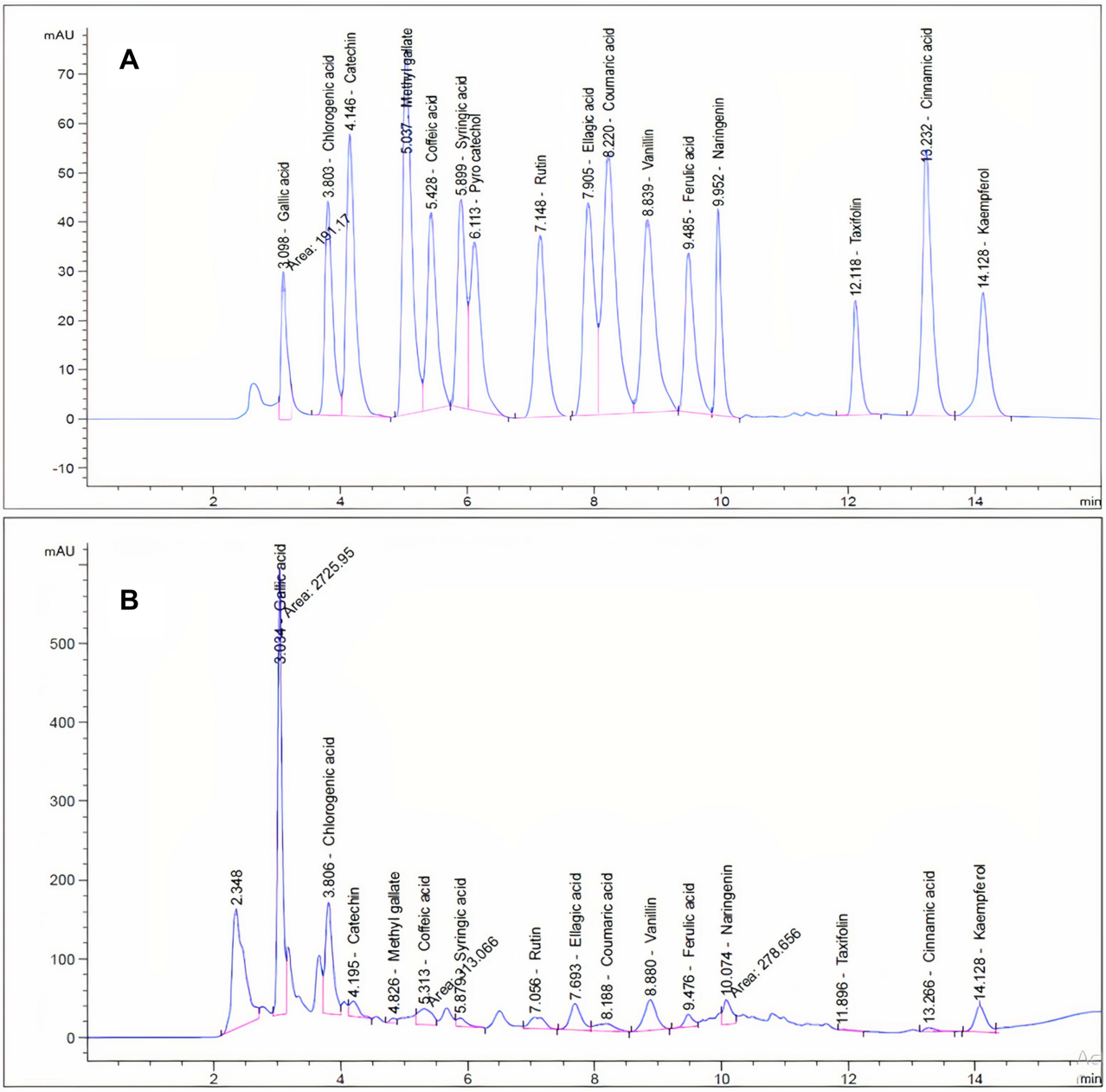

Figure 1 HPLC chromatogram: (**A**) standard mixture of polyphenolic compounds; (**B**) ethanolic extract of *P. indica* aerial parts.

shorter wavelengths than those found in standard ZnO, which is in parallel with the studies supporting the shorter wavelengths of material oxides.[45,46] The absorption of the ZnONPs in the UV region proves that the nanoparticles could be incorporated in various medical applications such as antiseptic ointments or sunscreen protectors.[47]

FT-IR Analysis of ZnONPs and *P. indica* L

The FTIR was analyzed in the range of 400 to 4000 cm^{-1} to identify the different functional groups present in the nanoparticles and *P. indica* extract. Regarding ZnONPs (Figure 4A), an intense absorption peak at 3457 cm^{-1} indicated the presence of the OH group responsible for the water adsorption on the ZnONP surface. Bands observed at 2925 and 2859 cm^{-1} related to the stretching vibration while the band existing at 913 cm^{-1} was assigned to the bending vibration of alkane groups. Absorption peaked at 1084 cm^{-1} signifying the occurrence of CO group of ethers, carboxylic acid esters and alcohols. The representative peaks of the ZnONPs were assigned at 524 and 493 cm^{-1}. FTIR spectrum for *P. indica* extract (Figure 4B) displayed a significant

Table 1 Polyphenolic Compounds of *P. Indica* L. Aerial Parts Identified by HPLC

No.	Compound	RT*	RRT*	Area	Conc. (µg/g)
1	Gallic acid	3.034	0.43	2725.95	8203.99
2	Chlorogenic acid	3.806	0.54	1159.31	2965.95
3	Catechin	4.195	0.59	193.11	792.42
4	Methyl gallate	4.826	0.68	36.21	16.83
5	Coffeic acid	5.313	0.75	313.07	458.24
6	Syringic acid	5.879	0.83	120.66	180.82
7	Rutin	7.056	1.00	245.62	1144.99
8	Ellagic acid	7.693	1.09	404.02	925.77
9	Coumaric acid	8.188	1.16	192.09	111.81
10	Vanillin	8.88	1.26	508.81	391.65
11	Ferulic acid	9.476	1.34	154.96	185.20
12	Naringenin	10.074	1.43	278.66	527.48
13	Taxifolin	11.896	1.69	9.87	24.58
14	Cinnamic acid	13.266	1.88	66.36	22.94
15	Kaempferol	14.128	2.00	404.00	542.65

Abbreviations: *RT, retention time; RRT, relative retention time to rutin.

peak at 3317 cm^{-1}, indicating the existence of phenolic or alcoholic OH groups. Medium bands observed at 2931 and 2830 $cm^{-}1$ revealed the incidence of alkane groups. The noticeable peaks at 1623, 1391 and 1334 cm^{-1} in the alcoholic extract indicated the existence of cyclic C–C or C=O stretch of polyphenolic compounds shifted to 1609 cm^{-1} in ZnONPs as a result of the bond between the polyphenols and NPs. The intense peak acquired at 1019 cm^{-1} proved the presence of alkane groups. The moderate bond that appeared at 730 cm^{-1} and the weak peaks at 894 cm^{-1} represented the alkenes (=C–H) group.[5,48]

Dynamic Light Scattering and Zeta Potential

The size distribution image (DLS) of green synthesized form of ZnONPs is shown in Figure 5A. The detected distribution of ZnONPs size varied from 15 to 94 nm. This nanoparticle's estimated average particle size distribution was 32.58 ± 7.98 nm. The stability of ZnONPs can be estimated by the zeta potential value. ZnONPs can be confirmed as stable colloidal solution when the absolute zeta potential is more than 30 mV.[49] The value of ZnONPs' zeta potential produced by *P. indica* was demonstrated as a clear peak at –20.8 mV (Figure 5B), signifying that the biosynthesized ZnONPs were negatively charged and moderately distributed in the medium.

Transmission Electron Microscope (TEM) and Scanning Electron Microscopy (SEM) Analyses

Low and high resolution transmission electron microscope (TEM) analysis showed the existence of ZnONPs in hexagonal shape and their corresponding range of particle size was between 2.56 and 8.83 nm (Figure 6A). The surface morphology of the obtained ZnONPs was visualized by scanning electron microscopy (SEM). The obtained image showed that most ZnONPs varied from spherical to hexagonal, with the particle diameter ranging from 19.64 to 23.21 nm (Figure 6B). SEM analysis illustrated the morphology and size of ZnONPs that was dispersed moderately in the medium. The relatively larger sizes observed by SEM were due to the smaller nanoparticle agglomeration.

XRD Analysis

The investigation of the structural features of ZnONPs was established through X-ray diffraction (XRD) (Figure 7). ZnONPs mediated by *P. indica* extract presented peaks with 2θ values recognized at 31.799°, 34.448°, 36.271°, 47.581°, 56.641°, 62.902°, 67.981°, 68.98°, and 72.751° corresponding to (100), (002), (101), (102), (110), (103), (200), (112), (201),

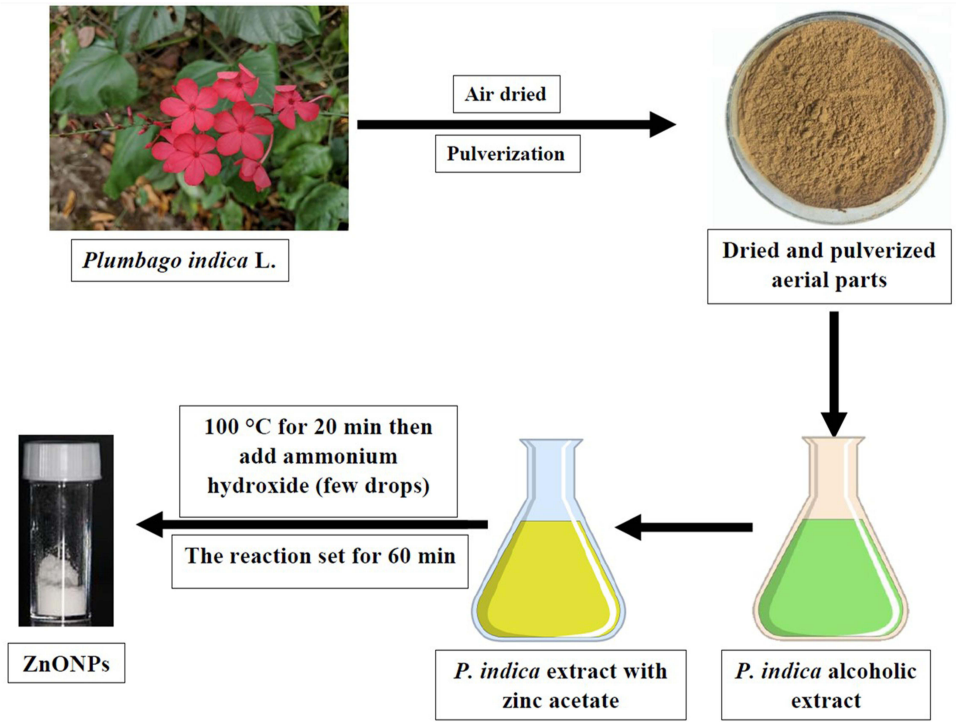

Figure 2 Schematic demonstration for the green synthesized ZnONPs mediated by the alcoholic extract of the aerial parts of *P. indica*.

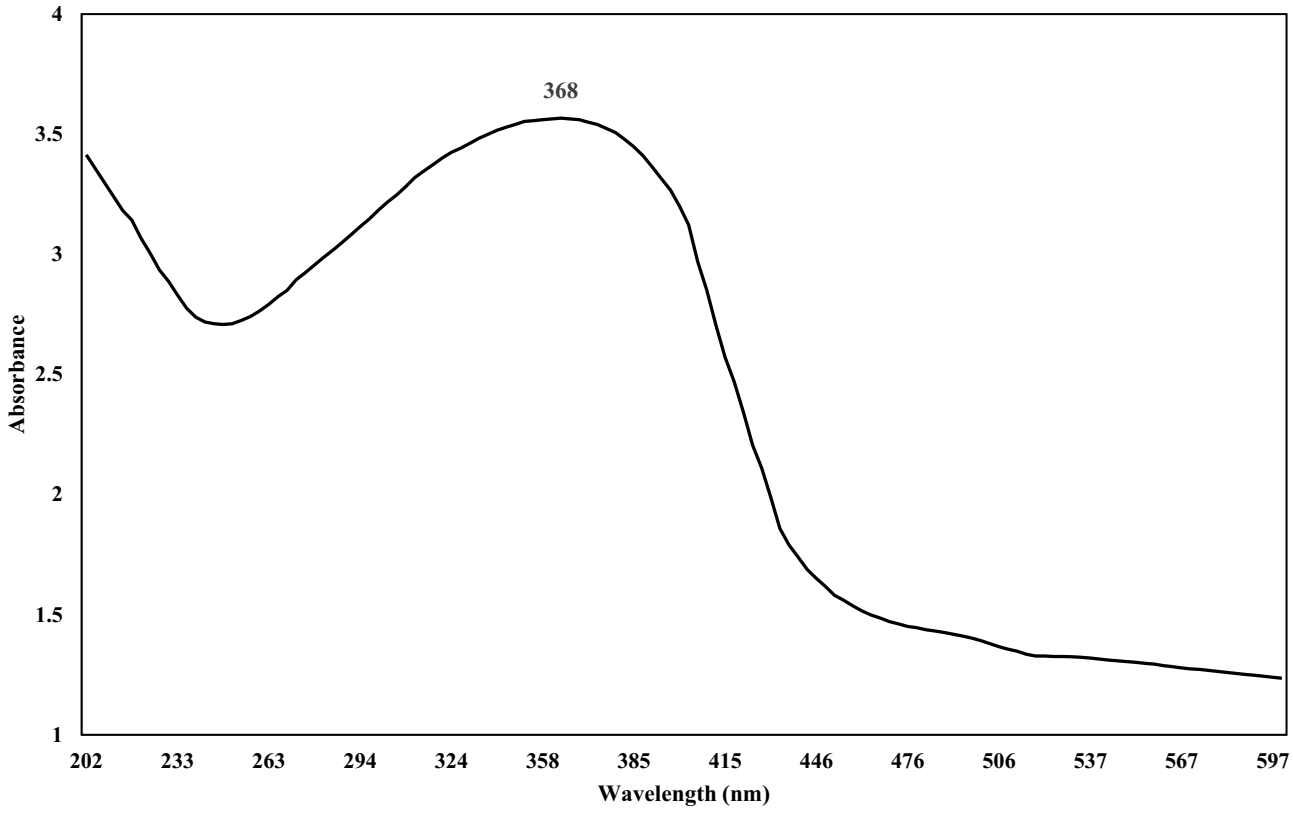

Figure 3 UV spectrum of biosynthesized ZnO nanoparticles.

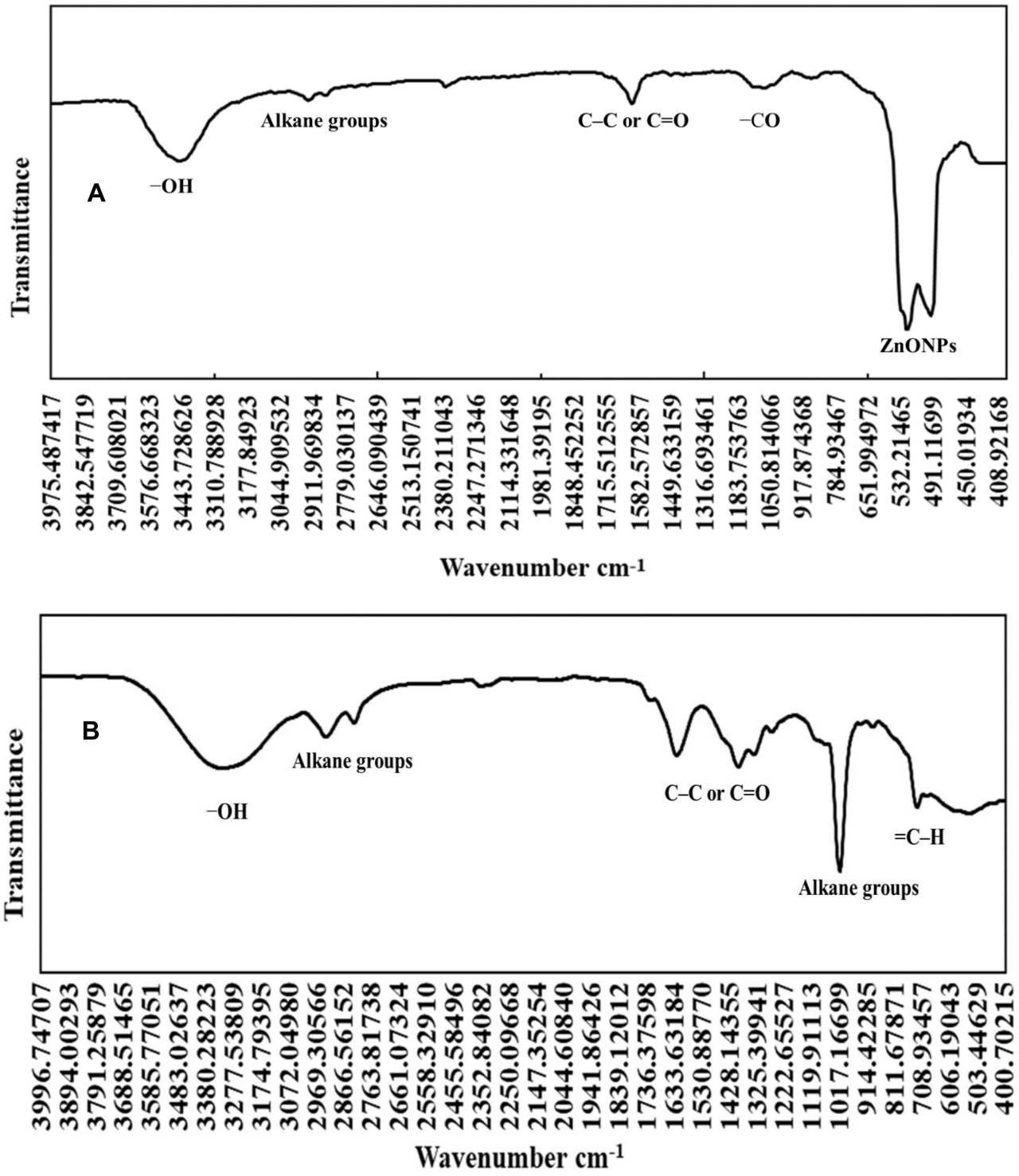

Figure 4 FTIR spectra of (**A**) the nanoparticles of ZnO; (**B**) the alcoholic extract of the aerial parts of *P. indica*.

(004). (202), (104), and (203), respectively. Furthermore, ZnONPs were considered impurity-free as there were no abnormal XRD peaks other than ZnONPs peaks.[46,50,51] These peaks are reported in crystal system of hexagonal phase with a space group of P63mc and reference code of (01-089-0510).

The average crystal size of ZnONPs was estimated to be 35.28 nm, very similar to SEM and DLS results.

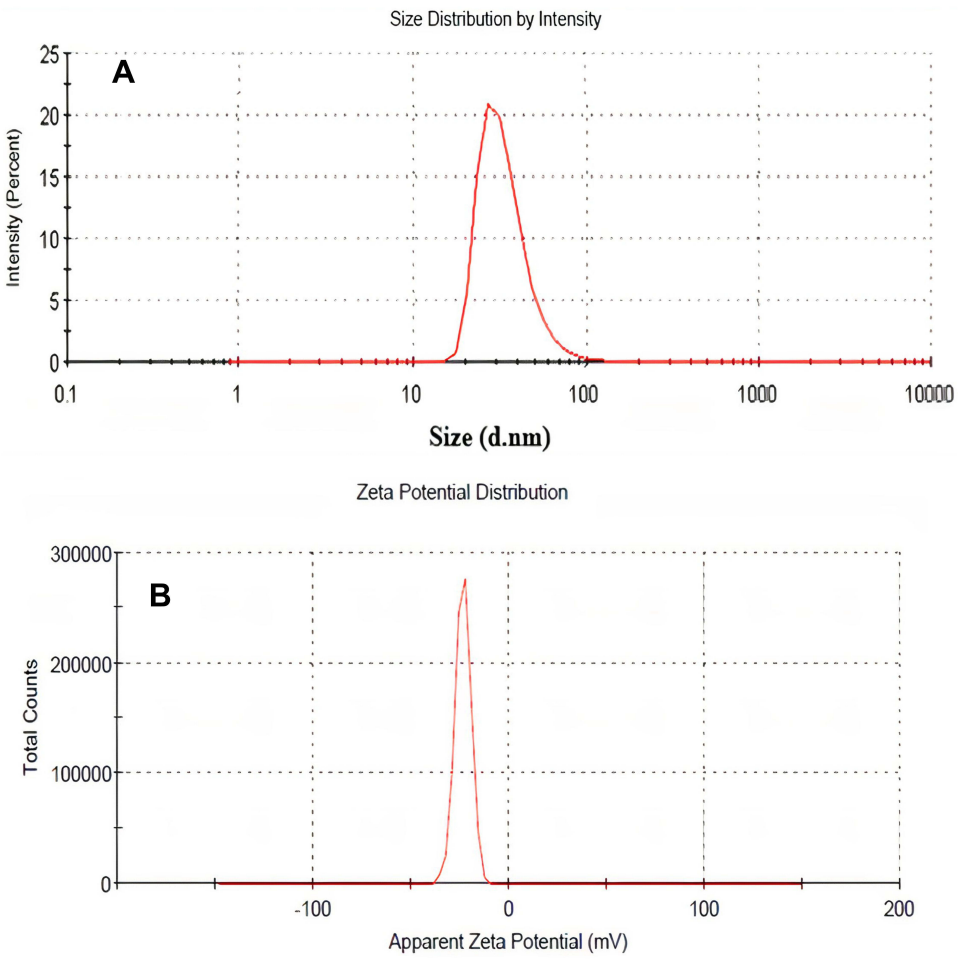

Figure 5 (**A**) DLS of biosynthesized zinc oxide nanoparticles; (**B**) zeta potential of biosynthesized zinc oxide nanoparticles.

To calculate the crystal size, Scherrer's equation was applied:

Crystal size = (0.9 x λ)/ (d cosθ) where; Θ = 2θ/2, d = the full width at half maximum intensity of the peak (in Rad), λ =0.154060 nm.

Cell Viability and Antiviral Activity Results of *P. indica* L. Extract and ZnONPs Concentrations (µg/mL)

HSV-1 and HSV-2 are two types of the herpes viridae family related to orolabial and genital infections. The in vivo studies recommended that Zn salts can be effective against the viral infection.[52,53] The first trial for employing nanoparticles as a candidates for an anti-HSV agent showed that a notable antiviral activity against HSV-1 in Vero cell line was observed in silver and gold NPs coated with mercapto ethane sulfonate.[54,55] ZnO micro-NPs covered with multiple nanoscopic spikes are considered a virostatic agent against HSV-1, while ZnO tetrapod micro-nanostructures is regarded as a prophylactic compound for the prevention of HSV-2 infection.[25,55]

The screening of the antiviral activities of *P. indica* L. extract and ZnONPs obtained by in vitro cell viability revealed that both agents displayed moderate inhibition. The observed medium percentages of cell destruction on Vero cell line were CC_{50}= 70.58 ± 4.32 and 43.96 ± 1.39 µg /mL, respectively. *P. indica* L. and ZnONPs exhibited anti-herpetic activity, with IC_{50}= 54.62 ± 1.53 and 23.1667 ± 2.2898 µg /mL, respectively, for MOI of 0.001 ID_{50} /cells. These results revealed that ZnONPs have better activity than the plant extract (Table 2). The antiviral activity of ZnONPs against HSV-1 could be due to direct interaction with the virus particles leading to trapping the virions followed by blocking the viral entrance into target cells. The selective inhibitory effect of Zn ions on viral

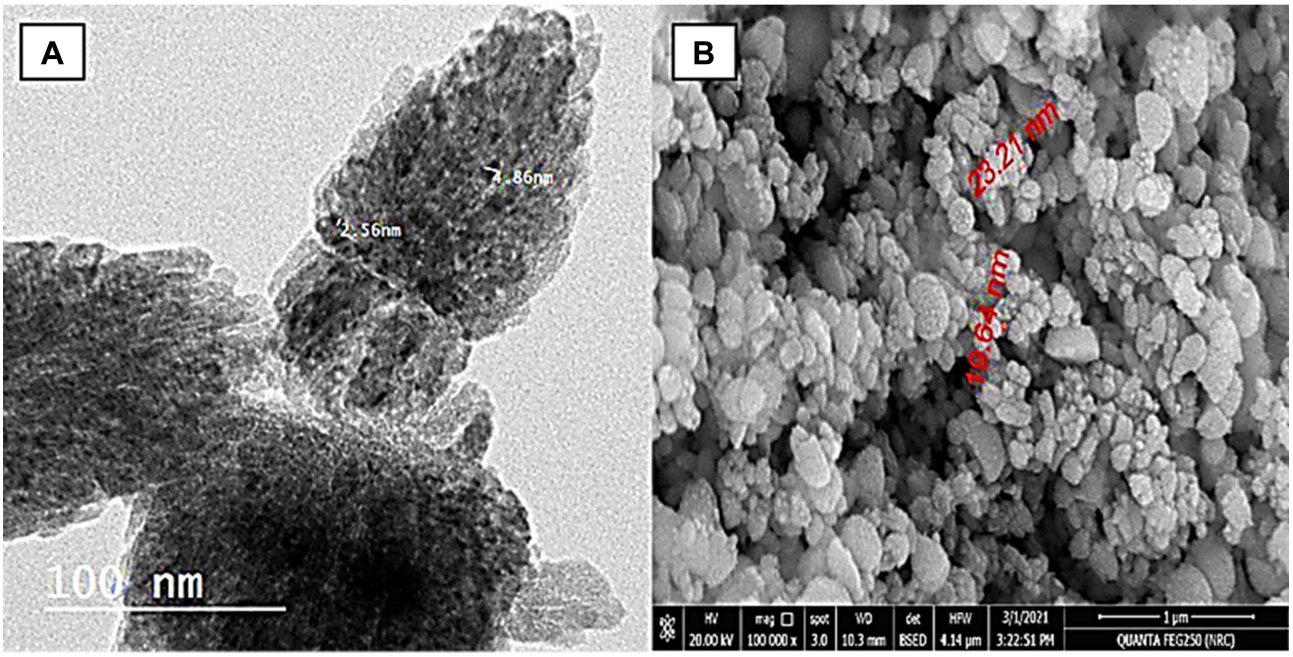

Figure 6 (**A**) TEM analysis of ZnONPs; (**B**) SEM analysis of ZnONPs.

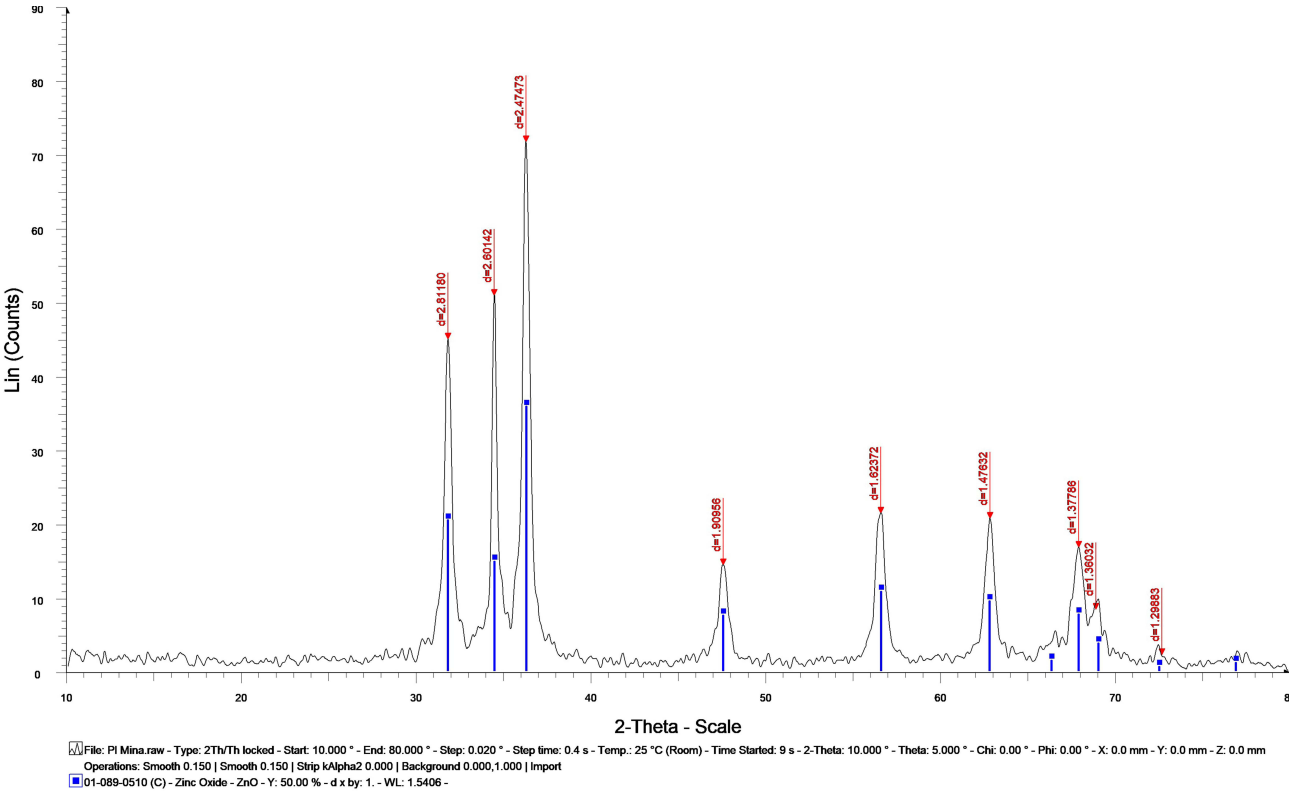

Figure 7 XRD analysis of ZnONPs.

Table 2 Anti-Herpetic (HSV-1) Activity of *P. Indica* Extract and ZnO Nanoparticles

	***Zovirax* (Positive Control)**		***P. indica***		**ZnO Nanoparticles**	
Species Mean ± SD	CC_{50}* >200 ± 0.2	IC_{50}* 0.5 ± 0.4	CC_{50}*@ 70.58 ± 4.32	IC_{50}*@ 54.6 ± 1.53	CC_{50}*@ 43.96 ± 1.39	IC_{50}*@ 23.17± 2.29

Notes: *Values are expressed as μg /mL, Mean ± SD. @Significantly different from positive control (*Zovirax*) group at $p<0.01$.

DNA polymerase leading to inhibition of HSV replication might be an alternative mechanism.[26] The antiviral activity of *P. indica* extract could be due to the active ingredients such as kaempferol that were previously found to have an antiviral property.[56]

In comparison to acyclovir, which provided 100% total protection against HSV-1 at 1 μg /mL, both *P. indica* extract and ZnONPs could be considered promising adjuvants to enhance the efficacy of HSV-1 drugs.

Conclusion

In this work, ZnONPs were successfully green synthesized by means of *P. indica* alcoholic extract. The resultant nanoparticles were characterized using DLS, zeta potential, UV–visible spectroscopy, FTIR, XRD, SEM and TEM. The antiviral activity of the ZnONPs was examined on herpes simplex virus – type 1. Our findings exposed that zinc oxide nanoparticles showed significant activity, higher than that of *P. indica* extract. This activity could be linked to its main small crystallite size (32.58 ± 7.98 nm), as indicated by XRD. The highest efficacy of *P. indica* alcoholic extract and ZnONPs synthesized from this extract might contribute to the search for new agents against HSV-1 or adjuvant with the standard antiviral drug, acyclovir.

Acknowledgments

The authors acknowledge Dr. Sedki Sedik Hasan Ahmed the associate Professor of English Language and Literature, Department of Foreign Languages, Faculty of Arts, Taif University for the English editing of the article.

Funding

This research funded by the Taif University Researchers Supporting Project number (TURSP-2020/81), Taif University, Taif, Saudi Arabia.

Disclosure

The authors declare no conflicts of interest in this work.

References

1. Waseem A, Divya K. Green synthesis, characterization and anti-microbial activities of ZnO nanoparticles using Euphorbia hirta leaf extract. *J King Saud Univ Sci*. 2020;32(4):2358–2364. doi:10.1016/j.jksus.2020.03.014
2. Seyyed M, Tabrizi HM, Behrouz E, Vahid J. Biosynthesis of pure zinc oxide nanoparticles using Quince seed mucilage for photocatalytic dye degradation. *J Alloys Compd*. 2020;821:153519.
3. Vijayakumar S, Arulmozhi P, Kumar N, Sakthivel B, Prathip kumar S, Praseetha PK. *Acalypha fruticose* L. leaf extract mediated synthesis of ZnO nanoparticles: characterization and antimicrobial activities. *Mater Today Proc*. 2020;23:73–80.
4. Muthuvel A, Jothibas M, Manoharan C. Effect of chemically synthesis compared to biosynthesized ZnO-NPs using Solanum nigrum leaf extract and their photocatalytic, antibacterial and *in vitro* antioxidant activity. *J Environ Chem Eng*. 2020;8(2):103705. doi:10.1016/j.jece.2020.103705
5. Niranjan B, Saha S, Chakraborty M, et al. Green synthesis of zinc oxide nanoparticles using Hibiscus subdariffa leaf extract: effect of temperature on synthesis, anti-bacterial activity and anti-diabetic activity. *RSC Adv*. 2015;5(7):4993–5003.
6. Yusof HM, Mohamad R, Zaidan UH, Rahman NAA. Microbial synthesis of zinc oxide nanoparticles and their potential application as an antimicrobial agent and a feed supplement in animal industry: a review. *J Anim Sci Biotechnol*. 2019;10(1):57. doi:10.1186/s40104-019-0368-z
7. Vidya C, Manjunatha C, Chandraprabha MN, Rajshekar M, Mal AR. Hazard free green synthesis of ZnO nano-photo-catalyst using Artocarpus Heterophyllus leaf extract for the degradation of Congo red dye in water treatment applications. *J Environ Chem Eng*. 2017;5(4):3172–3180. doi:10.1016/j.jece.2017.05.058
8. Vidya C, Manjunatha C, Sudeep M, Ashoka S, Raj MLA. Photo-assisted mineralisation of titan yellow dye using ZnO nanorods synthesised via environmental benign route. *SN Appl Sci*. 2020;2(4):1–15. doi:10.1007/s42452-020-2537-2
9. Cai L, Liu C, Fan G, Liu C, Sun X. Preventing viral disease by ZnONPs through directly deactivating TMV and activating plant immunity in Nicotiana benthamiana. *Environ Sci*. 2019;6(12):3653–3669.
10. Chaudhary A, Kumar N, Kumar R, Kumar R. Antimicrobial activity of zinc oxide nanoparticles synthesized from *Aloe vera* peel extract. *SN Appl Sci*. 2019;1(1):136. doi:10.1007/s42452-018-0144-2
11. Santhoshkumar J, Kumar SV, Rajeshkumar S, Adaikalaraj G. Synthesis of zinc oxide nanoparticles using plant leaf extract against urinary tract infection pathogen. *Resour Effic Technol*. 2017;3(6):459–1651. doi:10.1016/j.reffit.2017.05.001
12. Handago DT, Enyew AZ, Bedasa AG. Effects of Azadirachta indica leaf extract, capping agents, on the synthesis of pure and Cu doped ZnO-nanoparticles: a green approach and microbial activity. *Open Chem*. 2019;17(4):246–465. doi:10.1515/chem-2019-0018
13. Haque MJ, Bellah MM, Hassan MR, Rahman S. Synthesis of ZnO nanoparticles by two different methods & comparison of their structural, antibacterial, photocatalytic and optical properties. *Nano Express*. 2020;1(1):010007. doi:10.1088/2632-959X/ab7a43

14. El-Megharbel SM, Alsawat M, Al-Salmi FA, Hamza RZ. Utilizing of (zinc oxide nano-spray) for disinfection against "SARS-CoV-2" and testing its biological effectiveness on some biochemical parameters during (COVID-19 pandemic)—" ZnO nanoparticles have antiviral activity against (SARS-CoV-2)". *Coatings*. 2021;11(4):388. doi:10.3390/coatings11040388
15. Attia GH, Moemen YS, Youns M, Ibrahim AM, Abdou R, El Raey MA. Antiviral zinc oxide nanoparticles mediated by hesperidin and in silico comparison study between antiviral phenolics as anti-SARS-CoV-2. *Colloids Surf B Biointerfaces*. 2021;203:111724. doi:10.1016/j.colsurfb.2021.111724
16. Kurian A, Sankar MA. Medicinal Plants. Horticulture science series-2. KV Peter. New Delhi: New India Publishing Agency; 2007:123–143.
17. Priyanjani HASA, Senarath RMUS, Senarath WK, Munasinghe MLAMS. Propagation, phytochemistry and pharmacology of plumbago indica-a review. *ArticleGet*. 2021;33:188–202.
18. Melk MM, El-Hawary SSED, Melek FR, Saleh DO, Selim NM. Cytotoxic Plumbagin-5-O-α-l-Rhamnopyranoside from Plumbago indica. *Revista Brasileira de Farmacognosia*. 2021;75:1–4. doi:10.1007/s43450-021-00185-y
19. Mallavadhani UV, Sahu G, Muralidhar J. Screening of Plumbago species for the bio-active marker plumbagin. *Pharm Biol*. 2002;40:508–511. doi:10.1076/phbi.40.7.508.14685
20. Hazra B, Sarkar R, Bhattacharyya S, Ghosh PK, Chel G, Dinda B. Synthesis of plumbagin derivatives and their inhibitory activities against Ehrlich ascites carcinoma in vivo and Leishmania donovani promastigotes in vitro. *Phytopathol Res*. 2008;16:133–137.
21. Didry N, Dubreuil L, Pinkas M. Activity of anthraquinonic and naphthoquinonic compounds on oral bacteria. *Pharmazei*. 1994;49:681–683.
22. Kuo PL, Hsu YL, Cho CY. Plumbagin induces G2-M arrest and autophagy by inhibiting the AKT/mammalian target of rapamycin pathway in breast cancer cells. *Mol Cancer Ther*. 2006;5:3209–3322. doi:10.1158/1535-7163.MCT-06-0478
23. Wiesenthal A, Hunter L, Wang S, Wickliffe J, Wilkerson M. Nanoparticles: small and mighty. *Int J Dermatol*. 2011;50:247–254. doi:10.1111/j.1365-4632.2010.04815.x
24. Manjunatha C, Rao PP, Bhardwaj P, Raju H, Ranganath D. New insight into the synthesis, morphological architectures and biomedical applications of elemental selenium nanostructures. *Biomed Mater*. 2021;16(2):022010. doi:10.1088/1748-605X/abc026
25. Mishra YK, Adelung R, Rohl C, Shukla D, Spors F, Tiwari V. Virostatic potential of micro-nano filopodia-like ZnO structures against herpes simplex virus-1. *Antiviral Res*. 2011;92:305–312.
26. Tavakoli A, Ataei-Pirkooh A, Mm Sadeghi G, et al. Polyethylene glycol-coated zinc oxide nanoparticle: an efficient nanoweapon to fight against herpes simplex virus type 1. *Nanomedicine*. 2018;13 (21):2675–2690. doi:10.2217/nnm-2018-0089
27. Kumar TSJ, Balavigneswaran CK, Packiaraj RM, et al. Green synthesis of silver nanoparticles by plumbago indica and its antitumor activity against dalton's lymphoma ascites model. *BioNanoScience*. 2013;3:394–402. doi:10.1007/s12668-013-0102-9
28. Jaryal N, Kaur H. Plumbago auriculata leaf extract-mediated AgNPs and its activities as antioxidant, anti-TB and dye degrading agents. *J Biomater Sci Polym Ed*. 2017;28:1847–1858. doi:10.1080/09205063.2017.1354673
29. Govindan L, Anbazhagan S, Altemimi AB, et al. Efficacy of antimicrobial and larvicidal activities of green synthesized silver nanoparticles using leaf extract of Plumbago auriculata lam. *Plants*. 2020;9:1577. doi:10.3390/plants9111577
30. Roy A, Bharadvaja N. Silver nanoparticles synthesis from a pharmaceutically important medicinal plant Plumbago zeylanica. *MOJ Bioequi Availa*. 2017;3:46.
31. Maheswari T, Jayapriya G, Prabha N, Vennila M. Synthesis, Characterization and applications of selenium nanoparticle using Plumbago zeylanica leaves extract. *Plant Cell Biotechnol Mol Biol*. 2021;22:60–71.
32. Jamdade DA, Rajpali D, Joshi KA, et al. Gnidia glauca- and plumbago zeylanica-mediated synthesis of novel copper nanoparticles as promising antidiabetic agents. *Adv Pharmacol Sci*. 2019;2019:1–11.
33. Chopade BA, Salunke GR, Ghosh S, et al. Rapid efficient synthesis and characterization of silver, gold, and bimetallic nanoparticles from the medicinal plant Plumbago zeylanica and their application in biofilm control. *Int J Nanomed*. 2014;9:2635–2653. doi:10.2147/IJN.S59834
34. Maheswari T, Vennila M. Spectroscopic investigation of green and chemically synthesized zinc oxide nanoparticles and its antimicrobial activities. *IJSRR*. 2018;8:3363–3377.
35. Melk MM, El-Hawary SS, Melek FR, et al. Nano zinc oxide green-synthesized from plumbago auriculata lam. alcoholic extract. *Plants*. 2021;10(11):2447. doi:10.3390/plants10112447
36. Attia GH, Alyami HS, Orabi MAA, Gaara AH, El Raey MA. Antimicrobial activity of silver and zinc nanoparticles mediated by eggplant green Calyx. *Int J Pharmacol*. 2020;16:236–243. doi:10.3923/ijp.2020.236.243
37. Sayed AE-T, Salib JY, El- Kashak WA, Marty C, Bedoux G, Bourgougnon N. Antiviral effect of polyphenol rich plant extracts on herpes simplex virus type 1. *Food Sci Hum Wellness*. 2018;7:91–101.
38. Reed LJ, Muench HA. A simple method of estimating fifty per centendpoints. *Am J Hyg*. 1938;27:493–497.
39. Le Contel C, Galea P, Silvy F, Hirsch I, Chermann KC. Identification of the _2m-derived epitope responsible for neutralization of HIV isolates. *Cell Pharmacol AIDS Sci*. 1996;3:68–73.
40. McLaren C, Ellis MN, Hunter GA. A colorimetric assay or the measurement of the sensitivity of *Herpes simplex* viruses to antiviral agents. *Antivir Res*. 1983;3:223–234. doi:10.1016/0166-3542(83)90001-3
41. Langlois M, Allard JP, Nugier F, Aymard M. A rapid and automated colorimetric assay for evaluating in the sensitivity of *Herpes simplex* strains to antiviral drugs. *J Biol Stand*. 1986;14:201–211. doi:10.1016/0092-1157(86)90004-1
42. Harborne J. Plant polyphenols: occurrence of azalein and related pigments in flowers of *Plumbago* and Rhododendron species. *Arch Biochem Biophys*. 1962;96:171–178. doi:10.1016/0003-9861(62)90467-8
43. Srinivasan N, Rangasami C, Kannan JC. Synthesis structure and optical properties of zinc oxide nanoparticles. *Int J Appl Eng Res*. 2015;10:343–345.
44. Muhammad W, Ullah N, Haroon M, Abbasi BH. Optical, morphological and biological analysis of zinc oxide nanoparticles (ZnO NPs) using Papaver somniferum L. *RSC Adv*. 2019;9(51):29541–29548. doi:10.1039/C9RA04424H
45. Fakhari S, Jamzad M, Kabiri Fard H. Green synthesis of zinc oxide nanoparticles: a comparison. *Green Chem Lett Rev*. 2019;12:19–24. doi:10.1080/17518253.2018.1547925
46. Jena M, Manjunatha C, Shivaraj BW, Nagaraju G, Ashoka S, Aan MS. Optimization of parameters for maximizing photocatalytic behaviour of Zn1-xFexO nanoparticles for methyl Orange degradation using Taguchi and Grey relational analysis Approach. *Mater Today Chem*. 2019;12:187–199. doi:10.1016/j.mtchem.2019.01.004
47. Zak AK, Razali R, Abd Majid WH, Darroudi M. Synthesis and characterization of a narrow size distribution of zinc oxide nanoparticles. *Int J Nanomedicine*. 2011;6:1399. doi:10.2147/IJN.S19693
48. Yuvakkumar R, Suresh J, Saravanakumar B, Nathanael AJ, Hong SI, Rajendran V. Rambutan peels promoted biomimetic synthesis of bioinspired zinc oxide nanochains for biomedical applications. *Spectrochim Acta A Mol Biomol Spectrosc*. 2015;137:250–258. doi:10.1016/j.saa.2014.08.022

49. Chai MHH, Amir N, Yahya N, Saaid IM. Characterization and colloidal stability of surface modified zinc oxide nanoparticle. *J Phys Conf Ser*. 2018;1123(1):012007.
50. Bigdeli F, Morsali A, Retailleau P. Syntheses and characterization of different zinc (II) oxide nano-structures from direct thermal decomposition of 1D coordination polymers. *Polyhedron*. 2010;29:801–806. doi:10.1016/j.poly.2009.10.027
51. Kashyout AB, Soliman HMA, Shokry Hassan H, Abousehly AM. Fabrication of ZnO and ZnO: sb nanoparticles for gas sensor applications. *J Nanomater*. 2010;2010:341841. doi:10.1155/2010/341841
52. Fridlender B, Chejanovsky N, Becker Y. Selective inhibition of herpes simplex virus type 1 DNA polymerase by zinc ions. *Virology*. 1978;84(2):551–554. doi:10.1016/0042-6822(78)90274-X
53. Shlomai J, Asher Y, Gordon YJ, Olshevsky U, Becker Y. Effect of zinc ions on the synthesis of herpes simplex virus DNA in infected BSC-1 cells. *Virology*. 1975;66(1):330–335. doi:10.1016/0042-6822(75)90204-4
54. Baram-Pinto D, Shukla S, Perkas N, Gedanken A, Sarid R. Inhibition of herpes simplex virus type 1 infection by silver nanoparticles capped with mercaptoethane sulfonate. *Bioconjug Chem*. 2009;20(8):1497–1502. doi:10.1021/bc900215b
55. Baram-Pinto D, Shukla S, Gedanken A, Sarid R. Inhibition of HSV-1 attachment, entry, and cell-to-cell spread by functionalized multivalent gold nanoparticles. *Small*. 2010;6(9):1044–1050. doi:10.1002/smll.200902384
56. Lyu SY, Rhim JY, Park WB. Antiherpetic activities of flavonoids againstHerpes simplex virus type 1 (HSV-1) and type 2 (HSV-2) *in vitro*. *Arch Pharmacol Res*. 2005;28:1293–1301. doi:10.1007/BF02978215